高Ti,Nb析出强化高强钢接头强度及焊接热影响区软化行为分析

董现春, 张 楠, 陈延清, 张 熹*
(首钢技术研究院,北京 100043)

摘 要: 采用混合气体(80% Ar+20% CO_2)保护焊对高Ti,Nb析出强化高强钢进行了焊接强度试验研究. 结果表明,随着焊接热输入增大,接头强度有降低趋势. 焊接热影响区较母材硬度降低,存在软化行为. 粗晶区晶粒长大及10 nm以下(Ti,Nb,Mo)(C,N)第二相粒子的溶解造成强化效果降低. 未溶的(Ti,Nb,Mo)(C,N)第二相粒子固定了C,Mo元素,降低过冷奥氏体的稳定性,不能得到硬度较高的板条状马氏体或贝氏体,而形成硬度较低的粒状贝氏体. 第二相强化效果的降低不能通过组织强化有效弥补,从而造成粗晶区软化. 在细晶区热循环作用下,10 nm以下第二相粒子粗化,使得偏离其临界强化尺寸,析出强化效果降低,造成细晶区软化.

关键词: 析出强化; 高强钢; 接头强度; HAZ软化; 第二相粒子
中图分类号: TG156;TG457.11 文献标识码: A 文章编号: 0253-360X(2012)11-0072-05

董现春

0 序 言

抗拉强度700 MPa级以上的热轧高强度带钢中通常添加较高的Ti元素(质量分数0.07% ~ 0.15%)和Nb元素(质量分数0.02% ~0.08%). 轧制时在奥氏体高温区析出的(Ti,Nb)(C,N)第二相粒子阻滞奥氏体的再结晶过程,最终细化铁素体晶粒;相间析出或相变后在铁素体内形成的粒子非常细小,能产生强烈的析出强化效果. 第二相粒子的数量越多,质点越细小,其对强度的贡献越大,细小粒子(Ti,Nb)(C,N)(<10 nm)的强化作用显著[1].

高强钢在焊接热循环过程中所遇到的不可避免的问题是焊接热影响区晶粒粗化、焊接热循环造成的析出相的变化、从而引起热影响区的局部软化. 焊接热输入对热影响区软化影响明显,随着焊接热输入的增大,过热区组织在焊接热循环的作用下变化明显,焊接接头屈服强度逐渐降低[2]. 软化热影响区的屈服应力降低和宽度增加对接头的抗拉强度降低影响较大[3].

已有的报道对热影响区软化的工艺因素研究较多,有研究对含微量Ti元素(质量分数<0.03%)及微量Nb(质量分数<0.04%)处理钢中的第二相粒子在粗晶区焊接热循环中的变化,以及第二相粒子与粗晶区组织、韧性的关系作了系统论述[4-7],而对于高Ti元素(质量分数0.07% ~0.15%)和Nb元素(质量分数0.04% ~0.08%)中第二相粒子及热影响区软化行为的研究,尚未见相关报道. 作者针对具有热影响区软化特点的高Ti,Nb析出强化高强钢板进行系列试验,研究焊接热输入对焊接接头强度影响,探讨焊接接头强度的控制因素. 分析第二相粒子在焊接热循环过程的变化规律,探讨与焊接热影响区软化现象的联系.

1 试验方法

试验用钢板为工业生产的高Ti,Nb析出强化高强钢SQ700MCD,供货状态为热轧,厚度为10 mm. 焊接材料为NIMOCR气体保护实心焊丝. 试验材料化学成分和力学性能见表1和表2.

焊接设备为YD-500气体保护焊机,采用混合气体保护焊(80% Ar + 20% CO_2),气体压力0.5 MPa,流量20 L/min,焊丝伸出长度15 mm. 坡口角度为单面60°,1 mm钝边,预留2 mm间隙,打底焊道采用单面焊双面成形工艺,填充焊道采用5种热输入(表3):9 kJ/cm,11 kJ/cm,13 kJ/cm,16 kJ/cm,18 kJ/cm. 焊接前不预热(环境温度32 ℃),层间温度100 ~150 ℃. 采用WE-100拉力试验机对

收稿日期: 2012-05-23
* 参与此项工作的还有牟淑坤,张飞虎,生海

表 1　试验材料化学成分(质量分数，%)

Table 1　Chemical compositions of material investigated

试验材料	C	Si	Mn	P	S	Ni	Cr	Mo	Ti+ Nb	Fe
SQ700MCD 钢板	≤0.11	≤0.20	≤1.80	≤0.015	≤0.005	≤0.30	≤0.30	≤0.30	≤0.18	余量
NIMOCR 焊丝	0.09	0.57	1.56	0.010	0.013	1.35	0.25	0.25	—	余量

表 2　试验材料力学性能

Table 2　Mechanical properties of materials investigated

试验材料	屈服强度 R_{eL}/MPa	抗拉强度 R_m/MPa	断后伸长率 A(%)	冲击吸收功 A_{KV}/J
SQ700MCD 钢板	755	840	23	80(−20 ℃)(截面 7.5 mm×10 mm)
NIMOCR 熔敷金属	≥690	770 ~ 890	≥17	≥47(−40 ℃)(截面 10 mm×10 mm)

表 3　焊接工艺参数

Table 3　Parameters of welding

热输入 E/(kJ·cm^{-1})	焊接电流 I/A	电弧电压 U/V	焊接速度 v/(cm·min^{-1})	填充焊道数
9	200	23	30.6	2
11	220	25.5	30.6	2
13	237	28	30.6	2
16	237	28	25.2	1
18	237	28	21.6	1

接头进行横向拉伸性能测试. 采用 ZBC2452-3 冲击试验机检测接头各区域冲击吸收功. 采用 HVS-10Z 型维氏硬度计测试焊接接头各区域的硬度，加载力为 98 N.

母材及接头金相试样经研磨、抛光后，采用 4% 硝酸酒精腐蚀，在 OLYMPS 激光共焦显微镜上观察显微组织. 采取萃取-复型技术，在 JEM-2100F 透射电镜上观察母材及热影响区的第二相粒子.

2　试验结果及讨论

2.1　钢板组织及第二相粒子形貌

高强钢的金相组织(图 1)为铁素体+MA 岛，晶粒尺寸为 3 ~ 10 μm，硬度为 255 ~ 269 HV.

图 2a 为钢板中第二相粒子的典型 TEM 形貌，10 ~ 120 nm 粒子为球形和近长方形，晶内以及晶界上析出大量的 1 ~ 3 nm 粒子近椭球形. 限于电子束的直径，对 5 nm 以上的粒子进行能谱分析，图 2b 为母材中粒子(尺寸 6 nm)的 EDS 分析结果. 粒子中含有 Ti，Nb，Mo 三种合金元素，为(Ti，Nb，Mo)(C，N)强化相. 钢板强化类型为细晶强化+析出强化.

2.2　焊接接头力学性能

不同热输入接头横向抗拉强度如图 3 所示，焊接热输入为 9 ~ 11 kJ/cm 时，接头抗拉强度为 775 ~ 780 MPa，当热输入提高至 13 ~ 18 kJ/cm 时，接头强度为 750 ~ 760 MPa. 焊接接头的抗拉强度随热输入增大而降低. 焊缝和热影响区为接头的薄弱环节，屈服和断裂发生于焊缝和热影响区，断裂方式为塑性断裂.

表 4 为对接试板冲击吸收功，试样截面尺寸 7.5 mm×10 mm. 由表 4 看出在 9 ~ 18 kJ/cm 不同热输入下 SQ700MCD 焊接板的焊缝中心、熔合线、热影响区的−20 ℃冲击吸收功都能满足使用性能要求.

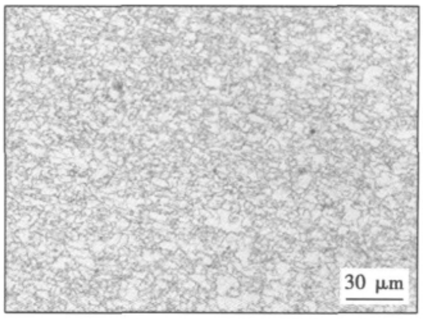

图 1　试验钢板组织

Fig. 1　Microstructure of test steel

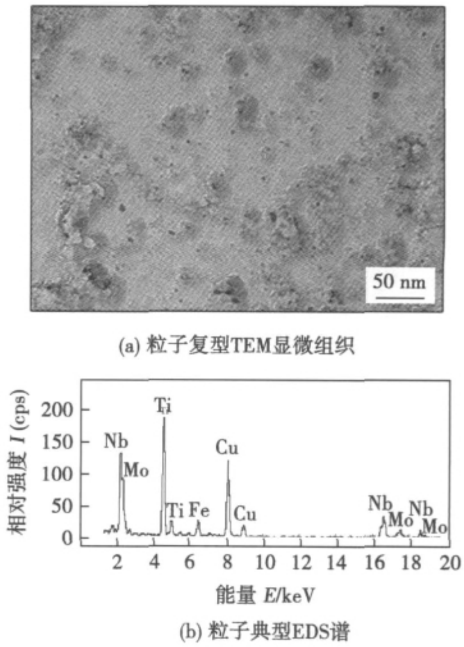

图 2　母材中第二相粒子

Fig. 2　TEM micrograph of second phase particle in steel

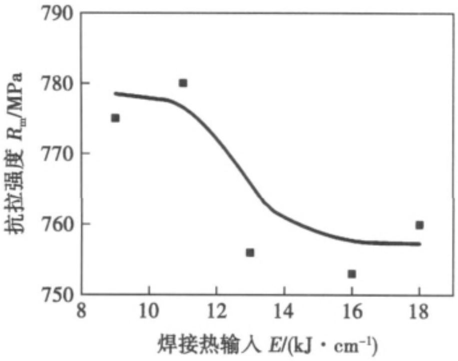

图3 接头抗拉强度与焊接热输入的关系

Fig. 3 Tensile strength of joint with different heat input

表4 对接试板冲击吸收功

Table 4 Charpy-type test of welding joint

热输入 $E/(\mathrm{kJ\cdot cm^{-1}})$	冲击吸收功 $A_{KV,-20\ ℃}$/J		
	焊缝中心	熔合线	热影响区
9	68	66	85
11	61	62	72
13	59	49	89
16	66	62	89
18	74	47	114

图4为硬度测试结果,可以看出焊接接头软化的区域包括热影响区的粗晶区、细晶区、不完全重结晶区;随焊接热输入的提高,软化程度和宽度均明显增大.

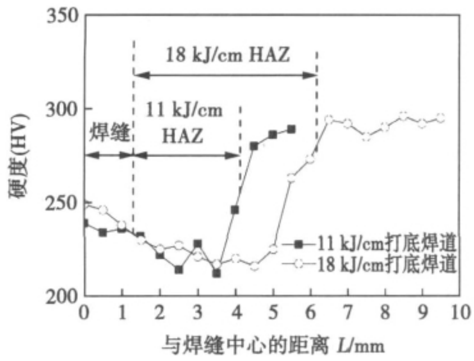

(a) 不同热输入接头打底焊道硬度

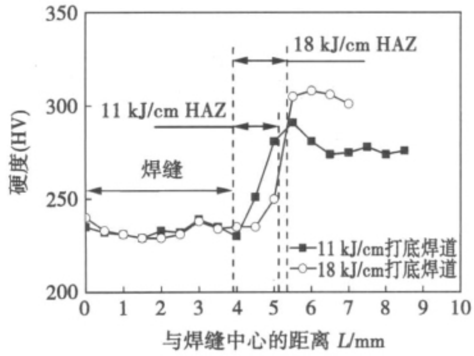

(b) 不同热输入接头盖面焊道硬度

图4 接头硬度

Fig. 4 Hardness profiles of welding joint

2.3 接头金相组织

图5为不同热输入焊缝显微组织,随着焊接热输入的提高,焊缝的针状铁素体比例降低,块状铁素体比例逐渐提高,硬度呈降低趋势.

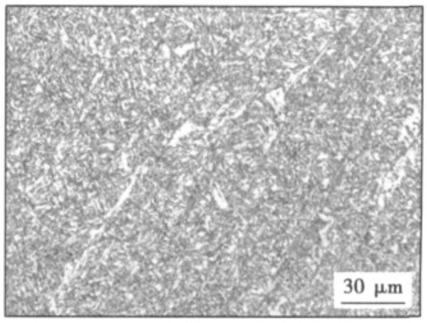

(a) 9 kJ/cm(242 HV)

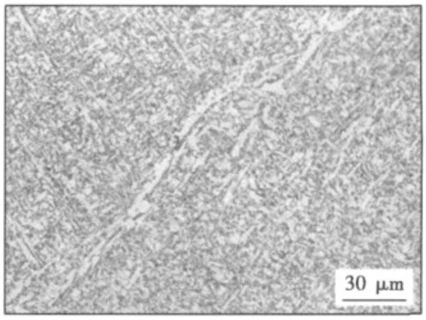

(b) 18 kJ/cm(222 HV)

图5 不同热输入焊缝显微组织

Fig. 5 Microstructure at FZ

图6为不同热输入粗晶区形貌,随着热输入的提高,焊接热影响区粗晶区从板条状为主的贝氏体组织逐渐向板条状贝氏体+粒状贝氏体的组织转变,硬度降低. 图7为不同热输入细晶区形貌,组织均为铁素体,晶粒尺寸2~8 μm,随着焊接热输入提高,晶粒尺寸提高为3~10 μm,而硬度呈降低趋势.

2.4 热影响区第二相粒子行为

图8为焊接热输入为18 kJ/cm的SQ700MCD粗晶区第二相粒子典型TEM形貌,统计结果显示,10 nm以下析出强化相全部溶解,析出强化效果消失,10~20 nm析出相部分溶解,而20 nm以上析出相则不溶解.

图9为焊接热输入18 kJ/cm的SQ700MCD细晶区第二相粒子典型TEM形貌,统计结果显示,最小析出相尺寸为3.28 nm,最大尺寸为1 339 nm,与母材相比,4~6 nm尺度的第二相粒子显著增多,而1~3 nm的第二相粒子减少.

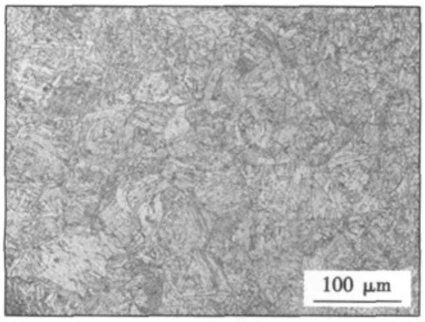

(a) 9 kJ/cm(246 HV)

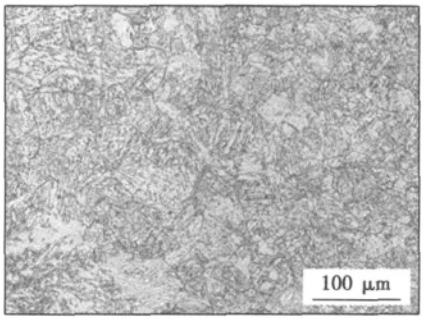

(b) 18 kJ/cm(233 HV)

图 6　不同热输入粗晶区显微组织
Fig. 6　Microstructure at CGHAZ

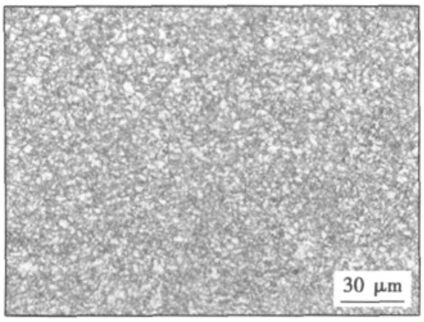

(a) 9 kJ/cm(228 HV)

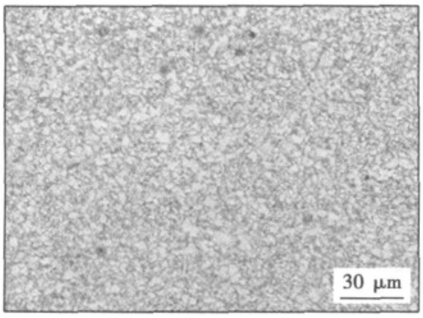

(b) 18 kJ/cm(226 HV)

图 7　不同热输入细晶区显微组织
Fig. 7　Microstructure at FGHAZ

对母材和焊接热影响区中的第二相粒子尺寸、粒子中 Ti，Nb，Mo 元素的相对比例进行了统计分析(图 10)，结果表明随着粒子尺寸增大，析出相中的

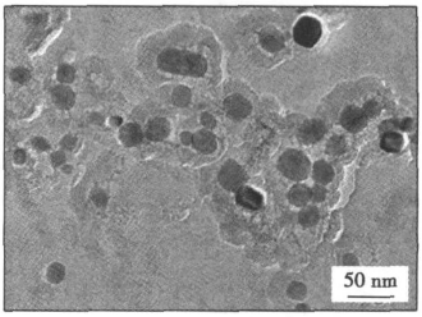

图 8　粗晶区第二相粒子
Fig. 8　TEM micrograph of second phase particle in CGHAZ

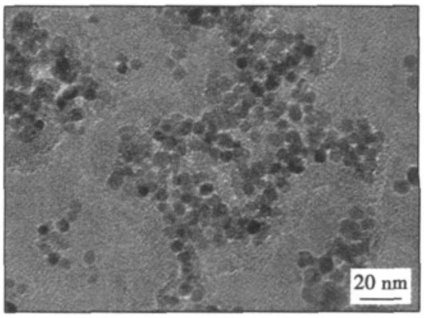

图 9　细晶区第二相粒子
Fig. 9　TEM micrograph of second phase particle in FGHAZ

Mo 元素相对比例降低，Nb 元素的相对比例增高，而 Ti 元素的相对比例介于 45% ~60% 之间.

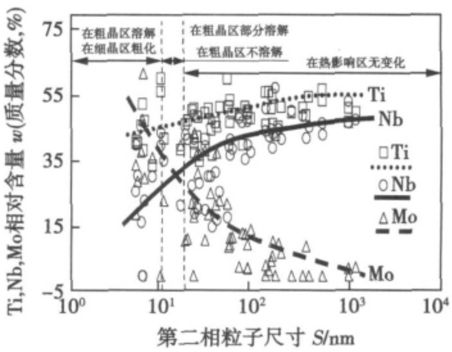

图 10　Ti，Nb，Mo 元素析出相对含量与第二相粒子尺寸关系
Fig. 10　Ratio analysis of Ti，Nb，Mo in second phase particle

在粗晶区中，未溶的第二相粒子固定了 C，Mo 等元素，降低粗晶区奥氏体的稳定性，使得粗晶区不能获得硬度较高的马氏体和板条状贝氏体. 细晶区中，10 nm 以下第二相粒子普遍长大粗化，偏离其理想强化临界尺寸(1 ~3 nm)，降低强化效果.

2.5　接头强度保证与热影响区软化分析

随着焊接热输入的提高，焊缝和热影响区的硬

度均低于母材，表明焊丝与母材为低强匹配，而焊接热影响区有软化现象. 在拉伸应力作用下，低强的接头发生塑性变形而开裂，从而使接头的抗拉强度低于母材. 说明此类型钢对热输入比较敏感. 采用较小的热输入可以有效提高接头的抗拉强度.

在焊接粗晶区热循环加热过程的高温阶段(1 200 ~ 1 350 ℃)，小尺寸第二相粒子大量消失，平均尺寸明显增大; 在冷却过程的高温阶段(1 350 ~ 1 300 ℃)，粒子仍继续溶解，其数量继续减少. 由于粗晶区在冷却速度较快，固溶状态的 Ti，Nb，Mo 与 C 元素重新结合并沉淀到残留较大(>20 nm) 粒子上，不能在析出敏感温度区间(600 ~ 950 ℃) 充分保温析出. 没有形成大量 1 ~ 3 nm 的第二相粒子，由此造成第二相强化效果的损失.

同时，由于 10 nm 以上的未溶(Ti，Nb，Mo)(C，N) 析出相固定了 C，Mo 元素，降低过冷奥氏体的稳定性. 随着焊接热输入的提高，$t_{8/5}$ 冷却时间延长，冷却速度降低，不能得到硬度较高的板条状马氏体或贝氏体，而形成硬度较低的粒状贝氏体. 第二相强化效果的消失不能通过组织强化有效弥补，从而造成粗晶区软化.

在焊接细晶区热循环过程中，产生的第二相的颗粒尺寸受其 Ostwald 熟化过程的影响，析出相在 600 ~ 950 ℃的升温和降温阶段发生未溶第二相的聚集长大. 10 nm 以下第二相粒子粗化，偏离其理想强化临界尺寸(1 ~ 3 nm)，使得析出强化效果降低，造成硬度及强度的降低.

3 结 论

(1) 高 Ti，Nb 析出强化高强钢热影响区的硬度低于母材硬度. 随着焊接热输入的提高，粗晶区的贝氏体内碳化物由板条状为主逐渐变为粒状为主，同时硬度也呈降低趋势; 细晶区的晶粒逐渐粗大，硬度也呈降低趋势. 此类型钢对热输入比较敏感，采用较小的热输入可以有效提高接头的抗拉强度.

(2) 高 Ti，Nb 析出强化高强钢为细晶强化+析出强化. 粗晶区中，10 nm 以下第二相粒子的溶解造成第二相强化效果降低. 未溶的(Ti，Nb，Mo)(C，N) 析出相固定了 C，Mo 元素，降低过冷奥氏体的稳定性，不能得到硬度较高的板条状马氏体或贝氏体，而形成硬度较低的粒状贝氏体. 第二相强化效果的降低不能通过组织强化有效弥补，从而造成粗晶区软化.

(3) 在细晶区热循环作用下，10 nm 以下析出相粗化，使得析出相偏离其临界强化尺寸，使得强化效果降低，造成细晶区强度硬度降低.

参考文献:

[1] 李杏娥，赵志毅，薛润东，等. Ti 在热轧高强带钢中的析出相与性能关系的研究[J]. 钢铁，2008，43(6): 70-73.
Li Xing'e，Zhao Zhiyi，Xue Rundong，*et al*. Study on relationship between precipitated phases containing Ti and properties of high strength hot strip[J]. Iron and Steel，2008，43(6): 70-73.

[2] 赵洪运，刘甲坤，骆宗安，等. 焊接热输入对 800 MPa 超级钢焊接接头组织性能的影响[J]. 焊接学报，2011，32(8): 5-8.
Zhao Hongyun，Liu Jiakun，Luo Zong'an，*et al*. Effects of welding heat input on structure and properties of 800 MPa ultra fine grained steel welding joints[J]. Transactions of the China Welding Institution，2011，32(08): 5-8.

[3] 朱 亮，陈剑虹. 热影响区软化焊接接头的强度及变形[J]. 焊接学报，2004，25(4): 61-65.
Zhu Liang，Chen Jianhong. Strength and deformation in HAZ-softened welded joints[J]. Transactions of the China Welding Institution，2004，25(04): 61-65.

[4] 陈茂爱，武传松，杨 敏，等. T-V-Nb 微合金钢第二相粒子在焊接热循环过程中的变化规律[J]. 金属学报，2004，40(2): 148-154.
Chen Maoai，Wu Chuansong，Yang min，*et al*. Response of second phase particles in Ti-V-Nb microalloyed steel during weld thermalcycles[J]. Acta Metallurgica Sinica，2004，40(2): 148-154.

[5] 陈茂爱，孙文涛，唐逸民，等. 焊接热循环对 Ti-V-Nb 微合金钢中第二相粒子的影响[J]. 机械工程学报，2000，36(10): 99-103.
Chen Maoai，Sun Wentao，Tang Yimin，*et al*. Effect of weld thermal cycle on particles in Ti-Nb-V microalloyed steel[J]. Chinese Journal of Mechanical Engineering，2000，36(10): 99-103.

[6] Fang Fang，Yong Qilong，Yang Caifu，*et al*. Microstructure and precipitation behavior in HAZ of V and Ti microalloyed steel[J]. Journal of Iron and Steel Research，International，2009，16(3): 68-72，77.

[7] Joonoh M，Changhee L. Behavior of(Ti，Nb)(C，N) complex particle during thermomechanical cycling in the weld CGHAZ of a micro-alloyed steel[J]. Acta Materialia，2009，57: 2311-2320.

作者简介: 董现春，男，1977 年出生，硕士，高级工程师. 主要从事高强钢材焊接性研究. 发表论文 10 余篇. Email: dongxianchun@shougang.com.cn

boundaries weakened. Impact toughness of the weld metal is not improved due to the boundaries of δ-ferrite are apt to become the crack sources when the weld metal is subjected to impact loads. Meanwhile, superior impact toughness is obtained by normalizing and tempering heat treatment for δ-ferrite is eliminated after the treatment and the weld metal of the joint transforms to tempered martensite which is the same to the base metal.

Key words: China low activation martensitic steel; vacuum electron beam welding; microstructure; impact toughness

Welded joint strength and analysis for HAZ softening behavior of high Ti and Nb precipitation strengthened high strength steel DONG Xianchun, ZHANG Nan, CHEN Yanqing, ZHANG Xi, MU Shukun, ZHANG Feihu, SHENG Hai (Shougang Research Institute of Technology, Beijing 100043, China). pp 72-76

Abstract: Welded joint's tensile strength of high Ti and Nb precipitation strengthing high strength steel with MAG(80% Ar+20% CO_2) was tested. The results show that the welded joint strength decreases with the increasing of the heat input. The hardness of the HAZ is lower than the base metal, and the HAZ has softening behavior. The growth of the grain and dissolution of the (Ti, Nb, Mo)(C, N) second phase particle (<10 nm) in CGHAZ weakend the precipitation strengthing. The particle without dissolution hold C and Mo, which weaken the stability of the overcooling austenite. The CGHAZ can not have lath martensite or bainite with high hardness, but has granular bainite with low hardness. The decreasing of the precipitation strengthing can not be balanced by structure strengthening, which leads to softening behavior in CGHAZ. The coarsing of the (Ti, Nb, Mo)(C, N) second phase particle (<10 nm) in FGHAZ, which offsets the critical size with best precipitation strengthing, weakened the precipitation strengthing, led to softening behavior in FGHAZ.

Key words: precipitation strengthing; high strength steel; welded joint strengthing; HAZ softening behavior; second phase particle

Influence of several times welding reworking on aluminum alloy welding joints for high speed train YU Jinpeng[1,2], ZHANG Limin[1], ZHANG Weihua[1], CHEN Hui[1], MA Jijun[2] (1. Traction Power State Key Laboratory, Southwest Jiaotong University, Chengdu 610031, China; 2. CNR Tangshan Co., Ltd, Tangshan 063035, China). pp 77-82

Abstract: One time, second time and third time welding reworking test were employed to test the EN 5083 welding joints. The morphology, hardness, tensile strength, impact toughness, cutting strength and push rate were analyzed. The results showed that the grains of the reworking layers were larger than the original welding layers. The α(Al)+β(Mg_2Al_3) net like morphology were much larger. The second phase after heated of the fusion area was much more than the original welding layers. The hardness, tensile strength, impact toughness were the same as the original welding layers. The cutting tongue of fracture was obviously which manifested the fracture mechanism was toughness. The cutting strength of the weld was lower but distributed stable. The cutting strength of different layers was the same as original which manifested the properties of the welding reworking layers were well. So the third reworking may be possible.

Key words: EN 5083 aluminum alloy; several times welding reworking; second phase; toughness fracture

Effect of energy arrangement on temperature field and stress field in dual-beam laser welding process with filler wire LEI Zhenglong[1], CHEN Yanbin[1], LV Tao[1], DIAO Wangzhan[1], SUN Zhongshao[2], CHEN Jilun[2] (1. State Key Laboratory of Advanced Welding and Joining, Harbin Institute of Technology, Harbin 150001, China; 2. Capital Aerospace Machinery Company, Beijing 100076, China). pp 83-88

Abstract: The heat source model of double-cylinder heat source + surface heat source is established in dual-beam laser welding process. Based on the finite element software Marc, the temperature field and stress-strain field of dual-beam laser welding with filler wire are simulated when the distance between two beams is 0.6 mm. And the effect of energy arrangement on the temperature characteristics and residual stress distribution are analyzed. The simulated results show that the heat melting efficiency decreases gradually with the decrease of the angle between the beam and the weld center. The residual stress mainly concentrate on longitudinal tensile stress in weld zone. At the same time, it can be found that the energy arrangement mainly affect the residual stress distribution and the angular deformation of the weld, while the effect on the maximum residual stress is not obvious.

Key words: Dual-beam laser welding; energy arrangement; temperature field; residual stress; numerical simulation

Soft-switch DC chopper four fold-frequency power control 300 KHz/50 kW induction welding power SHEN Jinfei, ZHAO Hui, YANG Lei (College of Electrical Engineering, Jiangnan University, Wuxi 214122, China). pp 89-92

Abstract: A four times frequency IGBT 300KHz induction welding power is put forward. Power control is composed with three-phase diode bridge inverter and DC chopper circuit. The chopper circuit adopts active nondestructive buffer buck converter , and in a wider range of the load the main, deputy switch tube and free-wheeling diode are achieve soft switch. The four groups of IGBT inverter in parallel are used for each IGBT in time-sharing control. The work frequency of the inverter is four times of the frequency IGBT switch. The inverter works in the load resonant state, and the switch tube works in shutting off at ZCS and switching on and off at ZVS. The output 300 kHz/50 kW serial-resonant inductive welding power was designed, and the design parameters and test waveforms were given. The results show that it is possible to produce capacity of high frequency induction heat welding power by using the method of four-times frequency control points with IGBT alternative power MOSFET.

Key words: induction welding; soft chopped; softswitch; fourfold frequency; time-sharing control

Effect of titanium on microstructure and properties of Zn-22Al filler metals YANG Jinlong[1], XUE Songbai[1], JI Feng[1], WANG Kebing[2], SUN Bo[2], Wang Shuiqing[2] (1. College of Materials Science and Technology, Nanjing University of Aero-